

## **Water Depth Effects on Fully Nonlinear Focused Waves**

**Xianglong Chen<sup>1</sup>, Wei Bai<sup>2\*</sup>, Paul Taylor<sup>3</sup>, Ser Tong Quek<sup>1</sup>, Ling Qian<sup>2</sup>, Jianguo Zhou<sup>2</sup>, Zhihua Ma<sup>2</sup>**

<sup>1</sup> Department of Civil and Environmental Engineering, National University of Singapore, Singapore

<sup>2</sup> School of Computing, Mathematics and Digital Technology, Manchester Metropolitan University, Manchester, UK

<sup>3</sup> Department of Engineering Science, University of Oxford, Oxford, UK

\* Present author: w.bai@mmu.ac.uk

### **1 INTRODUCTION**

There have been a number of publications discussing focused waves, their properties and mechanisms behind, but the available experiments and the relevant numerical simulations that particularly went deep into the water depth effects on focused waves are very rare. For this purpose, a series of numerical simulations are designed based on the fully nonlinear numerical model (Bai & Eatock Taylor, 2006), and the corresponding physical experiments are carried out to validate the accuracy of the numerical simulations. To investigate the nonlinear behaviors, the phase-inversion method (two-phase) described in Gibbs & Taylor (2005) has been widely used to separate the odd and even harmonics in the perturbation expansion. Siddorn (2012) used a combination of the time histories in phases  $0^\circ$ ,  $120^\circ$  and  $240^\circ$  to isolate the third order sum term without any contribution from the linear component. Fitzgerald et al. (2014) proposed a four-phase method to separate the harmonics of hydrodynamic forces using the linear combination of many time domain signals. In Hann et al. (2014), an alternative set of combinations of twelve wave groups was developed with phases shifted by  $30^\circ$  from  $0^\circ$  to  $330^\circ$ , in order to eliminate the need of frequency filtering as well as Hilbert transform. In the present analysis, the method similar to the work in Fitzgerald et al. (2014) is applied since this method provides an effective separation without requiring a large number of physical or numerical tests. The water depth effects on the focused waves, especially on the isolated harmonics, are discussed and analyzed. The effect of wave steepness is also taken into consideration in this study.

### **2 VALIDATION**

The physical experiment is carried out in the wave flume at the National University of Singapore (36m long and 2m wide). A number of surface-piercing wave gauges measuring the time history of wave elevation are installed over a span which covers the numerically predicted focal point. The wave is generated at the upstream end of the wave tank, by a piston-type wave paddle. At the downstream end of the wave tank, an effective passive absorber (consisting of polyether foam) is installed to avoid the wave reflection.

The JONSWAP spectrum ( $\gamma = 3.3$ ) is prescribed to the wave maker as the input signal with a frequency band of 0.48-1.00 Hz. Three water depths, 0.5m, 0.7m and 0.9m are considered in the experiment. The input wave steepness is defined as the local steepness of the focused wave crest. In each water depth, two wave steepnesses of 0.09 and 0.144 are considered. In order to avoid any confusion, the cases are named typically according to the parameters. The “EXP” stands for the experimental case and the “NUM” stands for the associated numerical case. The number affixing to them refers to as the water depth. The two wave steepnesses (0.09 and 0.144) are labeled with “stp1” and “stp2” respectively. Fig. 1 shows the comparisons of wave elevations between the numerical and experimental results in the water depths of 0.5m (a, d), 0.7m (b, e) and 0.9m (c, f). In each figure, the time histories of both the

crest-focused  $\eta(0)$  ( $0^\circ$  phase shift) and trough-focused  $\eta(180)$  ( $180^\circ$  phase shift) events are included. The fairly good agreements can be observed throughout all the comparisons in the time domain, which confirms the good accuracy of the present model in simulating focused waves with various wave conditions.

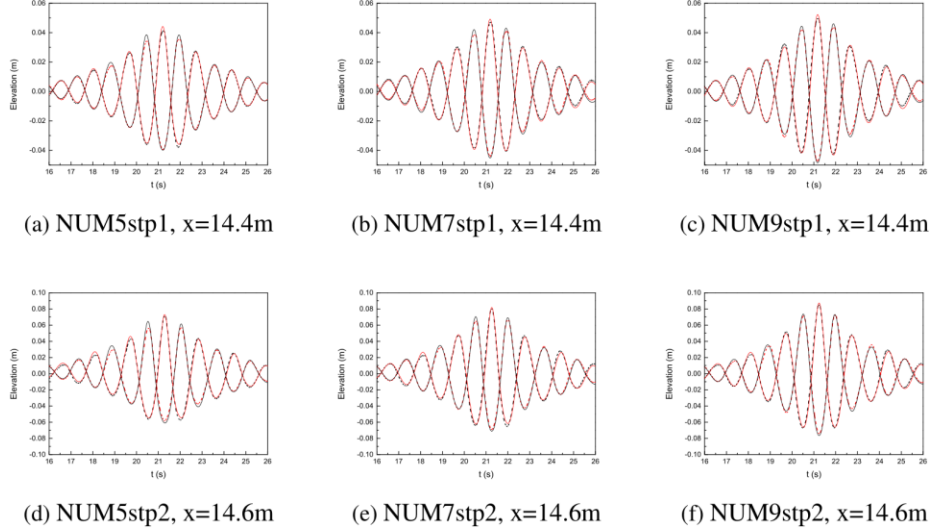


**Fig. 1 Comparisons of wave elevations between the numerical (solid line) and experimental (dash line) results for the crest-focused (black) and trough-focused (red) events: (a-c) wave steepness of 0.09; (d-f) wave steepness of 0.144.**

### 3 RESULTS AND DISCUSSION

For each case, four versions of the same wave group are generated as the incident waves and the Fourier components in the four versions are shifted by  $0^\circ$ ,  $90^\circ$ ,  $180^\circ$  and  $270^\circ$  respectively. The linear combinations of the four runs are expressed up to the fourth order as follows,

$$\frac{\eta(0) - \eta^H(90) - \eta(180) + \eta^H(270)}{4} = \eta_{11}A \cos \varphi + \eta_{31}A^3 \cos \varphi, \quad (1)$$

$$\frac{\eta(0) - \eta(90) + \eta(180) - \eta(270)}{4} = \eta_{22}A^2 \cos 2\varphi + \eta_{42}A^4 \cos 2\varphi, \quad (2)$$

$$\frac{\eta(0) + \eta^H(90) - \eta(180) - \eta^H(270)}{4} = \eta_{33}A^3 \cos 3\varphi, \quad (3)$$

$$\frac{\eta(0) + \eta(90) + \eta(180) + \eta(270)}{4} = \eta_{20}A^2 + \eta_{44}A^4 \cos 4\varphi, \quad (4)$$

where  $A$  is the wave amplitude,  $\varphi$  is the phase angle,  $\eta(0)$ ,  $\eta(90)$ ,  $\eta(180)$  and  $\eta(270)$  are the measured surface elevations in the four runs with four different phases, and  $\eta^H(90)$  and  $\eta^H(270)$  indicate the Hilbert transforms of  $\eta(90)$  and  $\eta(270)$ .

With the linear combinations presented in Eqs. (1-4), the harmonics up to the fourth order can be separated as shown in Fig. 2a. The first-order linear component is the predominant component compared with the other higher harmonics. The amplitude of the second-order sum harmonic is secondarily large among the harmonics and the third order sum harmonic follows it. It is interesting that the second-order difference long-wave is also fairly significant. If the separated signals in Fig. 2a

are transformed into the frequency domain, the separations are more straightforward and explicit as shown in Fig. 2b.

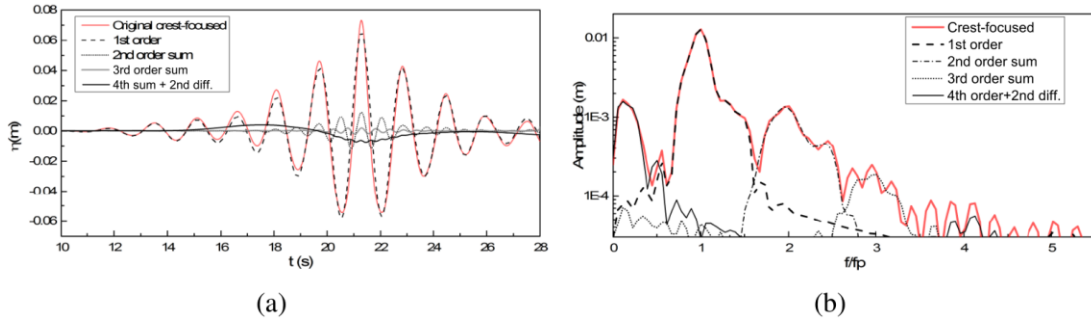


**Fig. 2** Time histories (a) and corresponding amplitude spectra (b) of the separated harmonics of Case NUM5stp2, and time histories and spectra of the original crest-focused event are also included.

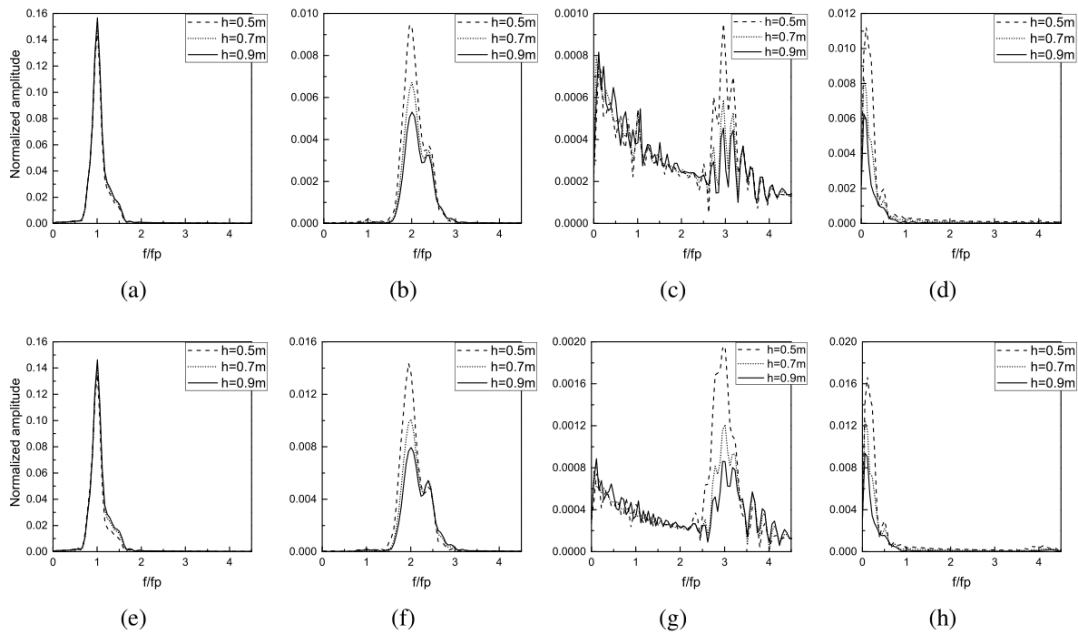


**Fig. 3** Amplitude spectra of separated harmonics at (a, e) first order, (b, f) second order sum, (c, g) third order sum and (d, h) fourth order + second order difference of numerical focused waves in different water depths: the first row for the input wave steepness of 0.09 and the second row for 0.144.

The same order harmonics resulted from the cases in different water depths are grouped in a series of plots as shown in Fig. 3. The figures in the upper row of Fig. 3 show the separated spectra of the first four harmonics of numerical cases in the wave steepness of 0.09. The first order harmonic does not change much with the water depth, while the differences over the water depth are relatively larger for the harmonics in higher orders as well as the subharmonics (i.e. second order difference harmonic). This makes sense because the spectra of all four components are normalized and the first order component provides the main contribution to the formation of the focused waves. Though the difference is small in Fig. 3a, it still indicates that the first order harmonic becomes more predominant relative to the other harmonics in the deeper water. However, the second order sum harmonic, the third order sum harmonic and the second order difference harmonic are more significant in the shallower water. The second order subharmonic is quite significant while the fourth order superharmonic is too

small to be viewed relative to the other components. The same behavior can be observed in the lower row of Fig. 3 which shows the cases with a larger input wave steepness of 0.144.

The four-phase approach (Eqs. 1-4) provides a way to evaluate the energy shares of the first four harmonics. Fig. 4 exhibits the comparisons for numerical cases with the wave steepnesses of 0.09 and 0.144 respectively. For the cases with the steepness of 0.09 in Fig. 4a, the energy share of the first order harmonic is increased by 7.71% when the water depth is changed from 0.5m to 0.9m. If the input wave steepness is 0.144 as shown in Fig. 4b, this value becomes 10.89%. In the shallower water, the superharmonics and the second order difference subharmonic can obtain more energy except for the third order harmonic. At the third order, the harmonic gets a small share of energy compared to the other harmonics, so that it is difficult to reveal a significant change of energy share in different water depths. If we look into the comparison between Fig. 4a and Fig. 4b, at the same order, the change of the energy share due to the wave depth is more remarkable if the input wave steepness is larger. In other words, the wave steepness of focused waves can magnify the water depth effect on the variation of energy shares occupied by different harmonics in nonlinear wave-wave interactions.

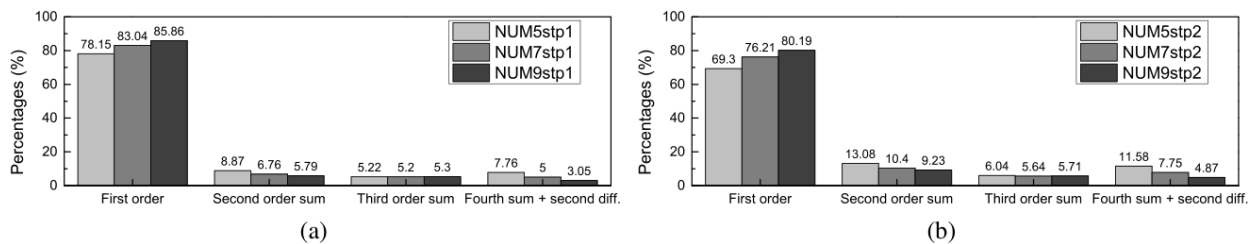


**Fig. 4 The distribution of wave energy contributed by the harmonics resulted from the four-phase separation method for numerical cases with the wave steepnesses of (a) 0.09 and (b) 0.144.**

## 4 CONCLUSION

In summary, the first order component is more predominant in the deeper water, while the second and third order superharmonics as well as the second order difference harmonic have more significant amplitudes in the shallower water even though the wave amplitude may be smaller in the shallower water for the same wave steepness. Considering the energy shares possessed by the first four harmonics in different water depths, it again confirms that the contributions of the other harmonics, especially the second order difference harmonic, cannot be neglected in the shallower water. It is also concluded that the wave steepness can magnify the water depth effect on the energy redistribution due to nonlinear wave-wave interactions.

## REFERENCES

- Bai, W., & Eatock Taylor, R. (2006). Higher-order boundary element simulation of fully nonlinear wave radiation by oscillating vertical cylinders. *Applied Ocean Research*, 28(4), 247-265.
- Fitzgerald, C., Taylor, P. H., Eatock Taylor, R., Grice, J., & Zang, J. (2014). Phase manipulation and the harmonic components of ringing forces on a surface piercing column. *Proceedings of the Royal Society of London A: Mathematical, Physical and Engineering Sciences*, 470(20130847), 1-21.
- Gibbs, R. H., & Taylor, P. H. (2005). Formation of walls of water in 'fully' nonlinear simulations. *Applied Ocean Research*, 27(3), 142-157.
- Hann, M., Greaves, D., & Raby, A. C. (2014). A new set of focused wave linear combinations to extract nonlinear wave harmonics. Paper presented at the 29<sup>th</sup> International workshop for water waves and floating bodies (IWWF).
- Siddorn, P. D. (2012). Efficient Numerical Modelling of Wave-Structure Interaction. Unpublished Ph.D. thesis, University of Oxford.